nature neuroscience

Visualizing APP and BACE-1 approximation in neurons yields insight into the amyloidogenic pathway

Utpal Das[1,2], Lina Wang[1,2], Archan Ganguly[1,2], Junmi M Saikia[2], Steven L Wagner[2], Edward H Koo[2,3] & Subhojit Roy[1,2]

Cleavage of amyloid precursor protein (APP) by BACE-1 (β-site APP cleaving enzyme-1) is the rate-limiting step in amyloid-β (Aβ) production and a neuropathologic hallmark of Alzheimer's disease; thus, physical approximation of this substrate-enzyme pair is a crucial event with broad biological and therapeutic implications. Despite much research, neuronal locales of APP and BACE-1 convergence and APP cleavage remain unclear. Here we report an optical assay, based on fluorescence complementation, for visualizing *in cellulo* APP–BACE-1 interactions as a simple on/off signal. Combining this with other assays tracking the fate of internalized APP in hippocampal neurons, we found that APP and BACE-1 interacted in both biosynthetic and endocytic compartments, particularly along recycling microdomains such as dendritic spines and presynaptic boutons. In axons, APP and BACE-1 were cotransported, and they also interacted during transit. Finally, our assay revealed that the Alzheimer's disease–protective 'Icelandic' mutation greatly attenuates APP–BACE-1 interactions, suggesting a mechanistic basis for protection. Collectively, the data challenge canonical models and provide concrete insights into long-standing controversies in the field.

Extracellular Aβ deposition is a pathologic hallmark of Alzheimer's disease and a central tenet of the decades-old amyloid cascade hypothesis positing that neuronal dysfunction, synapse loss, neurofibrillary degeneration and the full manifestation of Alzheimer neuropathology is initiated by Aβ. Aβ is generated by sequential cleavage of APP by the enzymes β- and γ-secretase, with BACE-1 cleavage being the rate-limiting step in this pathway[1]. Thus physical approximation of APP and BACE-1 is a required cell biological event in Aβ generation, and precise understanding of APP–BACE-1 interaction sites as well as pathways leading up to this approximation is vital.

Where do wild-type (WT) APP and BACE-1 meet, and what is the site of β-cleavage in neurons? Despite much research, the answer remains unclear[1]. A model favored at present is that after biogenesis in the Golgi both APP and BACE-1 recycle with the plasma membrane and converge in early endosomes, and that β-cleavage of APP occurs in early endosomal compartments[2–4]. However, several observations are inconsistent with this view, and it is unclear how the model applies to neurons—the relevant cell type in this case. First, at steady state, much of the WT APP and BACE-1 in neuronal and non-neuronal cell lines is located at the Golgi[5], and it is unclear why β-cleavage would be precluded there. Furthermore, APP and BACE-1 colocalize in multiple endocytic compartments in these cells, including both early and recycling endosomes[6]. Notably, existing models of the amyloidogenic pathway are almost entirely based on experiments in cells that lack the anatomy of neurons, which have elongated processes orders of magnitude longer than microscopic cell bodies. Anatomically and functionally distinct neuronal microdomains such as dendritic spines and presynaptic specializations are not considered in canonical models, and it is difficult to imagine that trafficking concepts that have emerged from studies in non-neuronal cells can be simply transferred to neurons.

In previous studies we visualized the trafficking of WT APP and BACE-1 in cultured hippocampal neurons using minimal and transient expression of fluorescently tagged proteins[7]. We found that in dendrites, BACE-1 is largely localized to recycling endosomes, where APP and BACE-1 can colocalize. However, neuronal sites of APP–BACE-1 interaction and β-cleavage have remained unknown. Moreover, putative APP–BACE-1 interactions in axons and presynaptic sites were also not addressed. Here we report a tool we call the optical convergence of APP and BACE-1 (OptiCAB) assay that allows one to directly visualize APP–BACE-1 interactions in cells. Combining this with other assays that track the fate of internalized APP from the plasma membrane, as well as two-color high resolution live imaging, our experiments offer concrete insights into long-standing questions and controversies in the field.

RESULTS

Characterization of the OptiCAB assay

The OptiCAB assay is based on fluorescence complementation of Venus protein fragments (called bimolecular fluorescence complementation, or BiFC), an established tool for visualizing protein-protein interactions[8]. In this assay, one partner of an interacting pair is tagged with the N terminal fragment of the Venus fluorescent protein (VN), while the other partner is tagged with the complementary C terminus (VC). Although individual the VN and VC fragments are nonfluorescent, Venus is reconstituted and becomes fluorescent if and when the two interacting partners bind. We tagged the C terminus of WT APP and BACE-1 with VN and VC, respectively, following

[1]Department of Pathology, University of California, San Diego, La Jolla, California, USA. [2]Department of Neurosciences, University of California, San Diego, La Jolla, California, USA. [3]Department of Medicine and Physiology, National University of Singapore, Yong Loo Lin School of Medicine, Singapore. Correspondence should be addressed to U.D. (udas@ucsd.edu) or S.R. (s1roy@ucsd.edu).

Received 21 February; accepted 4 November; published online 7 December 2015; doi:10.1038/nn.4188

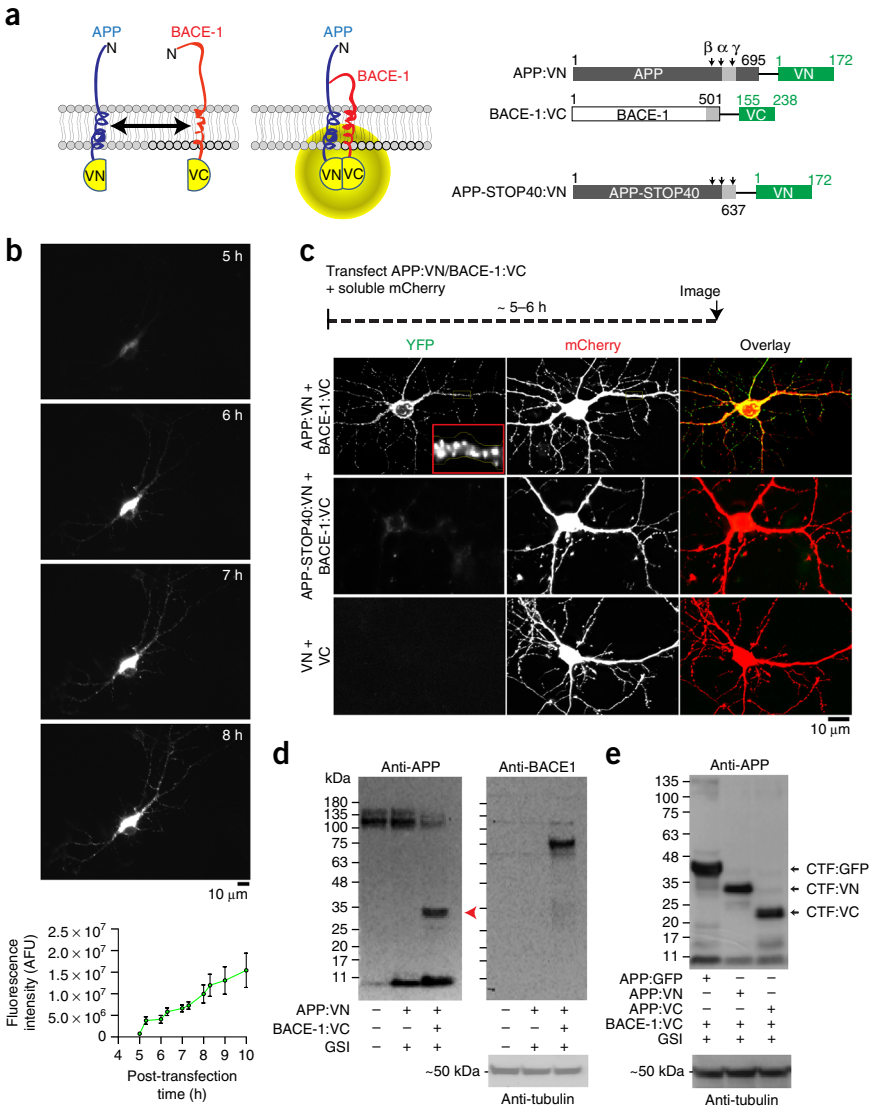

Figure 1 OptiCAB: an assay to detect APP–BACE-1 interactions *in situ*. (**a**) The principle: APP and BACE-1 are tagged to complementary (VN- or VC-) fragments of VFP. Interaction of APP with BACE-1 leads to reconstitution of VFP fluorescence. Cloning strategies on right; numbers denote amino acid residues and light gray box represents the transmembrane domain. (**b**) Hippocampal neurons were cotransfected with APP:VN and BACE-1:VC, and time course of complementation was evaluated. Time after transfection (in hours) shown on upper right; intensities quantified below ($N = 7$ neurons). Note the gradual increase in somatic and neuritic fluorescence over time. AFU, arbitrary fluorescence units; error bars are mean ± s.e.m. (**c**) Neurons transfected with APP:VN/BACE-1:VC and cytosolic mCherry; note punctate fluorescence in soma and dendrites (top panels, zoomed in inset). Attenuated complementation was seen with an APP C-terminal mutant (APP-STOP40, middle panels). Individually transfected VN and VC fragments were nonfluorescent (bottom panels). (**d**) Cleavage of APP:VN by BACE-1:VC. BACE-1 knockout fibroblasts were transfected with APP:VN alone or APP:VN plus BACE-1:VC (with a γ-secretase inhibitor (GSI)), and APP cleavage products were analyzed by western blotting. In the presence of BACE-1:VC, APP:VN was cleaved to generate a fragment of ~30 kDa (red arrowhead)—the expected β-cleavage product of APP:VN. Corresponding BACE-1 blot confirms knockdown. (**e**) Neuro2A cells were cotransfected with APP (APP:GFP, APP:VN or APP:VC) and BACE-1:VC in presence of a GSI and APP-cleavage products were analyzed by western blotting. The main bands are consistent with CTF:GFP (~40 kDa), CTF:VN (~30 kDa) and CTF:VC (~22 kDa), indicating that β-cleavage is not influenced by APP–BACE-1 complementation.

previously established tagging strategies (**Fig. 1a**; see Online Methods and ref. 7 for details). An advantage of this assay is that complementation is irreversible, 'capturing' transient interactions, and indeed this assay has been validated for several enzyme-substrate pairs (for instance, see refs. 9,10).

First we transfected mature cultured hippocampal neurons with well-developed spines (days *in vitro* (DIV) 10–14, isolated from postnatal mouse pups) with APP tagged with VN and BACE-1 tagged with VC (APP:VN/BACE-1:VC) and with volume-filling mCherry, examining the cells thereafter. Fluorescence was first visible ~5 h after expression, appearing in the soma and then along processes (**Fig. 1b**). On the basis of this observation, we decided to examine our neurons ~5–6 h after APP:VN/BACE-1:VC transfection (**Fig. 1c**). At these early times the fluorescent proteins are just starting to fold and mature, and protein expression levels are at a minimum. Thus it is unlikely that conclusions based on these experiments are confounded by overexpression artifacts (also see data with the 'broken promoter' below). APP:VN/BACE-1:VC fluorescence in dendrites was punctate, resembling vesicles (**Fig. 1c**).

Several observations argue that the fluorescence read-out of the OptiCAB assay is a consequence of APP–BACE-1 interactions and not nonspecific association of the Venus fragments. The best way to determine specificity is to mutate one interacting partner in a BiFC pair and ask whether the fluorescence complementation is attenuated. To this end, we engineered an APP-fragment containing the β-cleavage site and membrane-spanning domain but lacking the C terminus, suspected to mediate APP–BACE-1 associations (called APP-STOP40; see ref. 11). Neurons transfected with APP-STOP40:VN and BACE-1:VC were essentially nonfluorescent (**Fig. 1c**). Individually transfected VN or VC fragments were also nonfluorescent (**Fig. 1c** and data not shown). These results are not due to variable expression of the transfected constructs as all tested constructs expressed adequately in neurons (**Supplementary Fig. 1a**). Further data shown below (APP:VN-cleavage by BACE-1:VC and effects of Alzheimer's disease mutants) also strongly argue for the specificity of APP–BACE-1 interactions in our assay.

Does fluorescence complementation of APP:VN and BACE-1:VC lead to the cleavage of APP:VN? To address this, we cotransfected APP:VN and BACE-1:VC into cell lines, blocking γ-secretase activity with the inhibitor BMS-299897, and analyzed APP cleavage products by western blotting. If the APP:VN protein was cleaved by BACE-1:VC in these experiments, one would expect to see a cleaved APP β-C-terminal fragment (β-CTF) linked to the 17–19 kDa VN protein (β-CTF:VN), as the γ-secretase inhibitor would block further processing

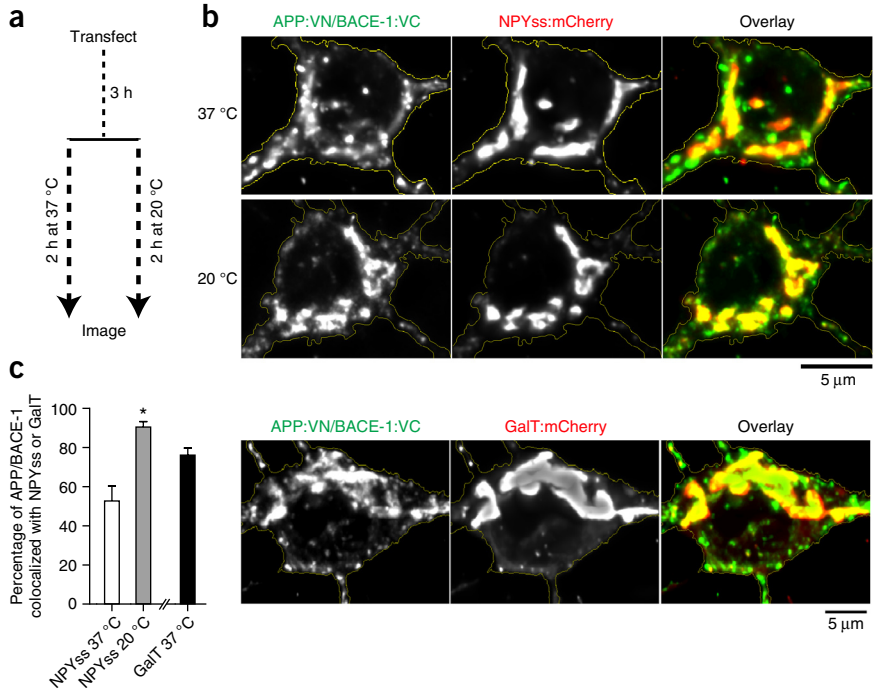

Figure 2 APP–BACE-1 interactions in the *trans*-Golgi network. (**a**) Hippocampal neurons were cotransfected with APP:VN/BACE-1:VC (to mark APP–BACE-1 interaction sites) and NPYss-mCherry (to label Golgi-derived organelles), and a subset of neurons were incubated at 20 °C, a condition known to trap vesicles at the TGN. (**b**) Colocalization of complemented APP–BACE-1 puncta with NPYss, enhanced upon temperature block. Complemented APP–BACE-1 also extensively colocalized with the TGN marker GalT. (**c**) Quantification of fluorescence intensities. Colocalization of complemented APP–BACE-1 with NPYss at 20 °C increased to 90.44 ± 2.81% from 52.68 ± 7.62% at 37 °C; $^*P = 0.0002$, unpaired *t*-test, $n = 11$ neurons for each group from two separate sets of cultures; error bars are mean ± s.e.m.

of this fragment. To eliminate potentially confounding effects of endogenous BACE-1, we first performed these experiments in a fibroblast cell line lacking BACE-1, generated from *Bace1*$^{-/-}$ mice. Cleavage of APP:VN by BACE-1:VC generated an expected ~30-kDa fragment consistent with β-CTF:VN (**Fig. 1d**). Similar results were obtained from neuro-2A cells (**Fig. 1e**). Furthermore, cleavage patterns of various APP constructs also suggested that complementation does not influence β-cleavage (**Fig. 1e**), and omission of the γ-secretase inhibitor led to the expected shifts in APP cleavage (**Supplementary Fig. 1b**). Also, APP mutants linked to familial Alzheimer's disease ('Arctic' and 'London' mutations, known to enhance APP β-cleavage; see refs. 12,13) led to the expected increases in β-CTF levels in the OptiCAB assay, though total fluorescence was not enhanced in the short time frames examined (4–6 h; **Supplementary Fig. 2a**,**b**).

APP–BACE-1 interaction sites in somatodendritic domains

Precise sites where APP and BACE-1 meet within neurons are unknown. Previous studies in non-neuronal cells or neuronal cell lines implicate a variety of locales, including the endoplasmic reticulum, Golgi, endosomes (early, late and recycling) and lysosomes[14]. The OptiCAB assay offers an opportunity to pinpoint APP–BACE-1 interaction sites in neurons. Our general strategy was to localize WT APP–BACE-1 interaction sites unambiguously by fluorescence complementation in hippocampal neurons and determine its colocalization with established organelle markers. Somatic APP:VN/BACE-1:VC fluorescence was perinuclear, consistent with a *trans*-Golgi network (TGN)-type distribution. To confirm this, we cotransfected neurons with APP:VN plus BACE-1:VC, to label interaction sites, and neuropeptide Y signal sequence (NPYss), a marker that labels the interior of Golgi and Golgi-derived organelles[15,16]. A subset of neurons was incubated at 20 °C for 2 h to block the export of proteins from the TGN (**Fig. 2a**). The colocalization of complemented APP:VN/BACE-1:VC with NPYss was augmented after the temperature block (**Fig. 2b**). Furthermore, complemented APP/BACE-1 also colocalized with galactosyl transferase (GalT), a marker of TGN, confirming APP–BACE-1 interactions at this locale (**Fig. 2b**,**c**).

Next we focused on dendrites. Punctate structures representing APP–BACE-1 interactions were seen throughout the dendritic profiles, including shafts and spines (**Fig. 3a**). Notably, ~80% of the APP–BACE-1 complementation was seen in and around dendritic spines (**Fig. 3b**), suggesting a role for these specialized recycling microdomains in APP β-cleavage. To determine specific organelles where APP and BACE-1 interact, we cotransfected neurons with APP:VN plus BACE-1:VC and various established organelle markers (transferrin receptor (TfR) and Rab11 for recycling endosomes, Rab5 for early endosomes, LAMP-1 for late endosomes or lysosomes, and NPYss for Golgi-derived vesicles; also see ref. 7) and analyzed the neurons after ~5–6 h (**Fig. 3c**). Complemented APP/BACE-1 most conspicuously colocalized with recycling endosome markers (~60% colocalization with TfR and Rab11, as opposed to ~20–30% with other markers; **Fig. 3c**,**d**). In previous studies, we and others found that, at steady state, neuronal BACE-1 is largely localized to recycling endosomes[7,17]. A role for endocytosis in APP processing is well established[18], and, on the basis of experiments evaluating the trafficking of APP and BACE-1 by live imaging, we proposed a model whereby APP undergoes endocytosis and meets BACE-1 in recycling endosomes[7]. Consistent with this model, we found that APP–BACE-1 complementation was attenuated upon inhibition of APP endocytosis—either directly, by mutation of a C-terminal APP endocytosis motif (YENPTY; see ref. 19), or by a global inhibition of endocytosis by the dynamin-inhibiting agent Dynasore (**Fig. 3e**). These data are unlikely to be a consequence of overexpression, as an APP/BACE-1 construct driven by weakened promoters lacking enhancer elements ('broken CMV promoter'; see ref. 20) also gave similar results (**Supplementary Fig. 2c**,**d**).

APP–BACE-1 interaction sites in axons and presynapses

Next we studied WT APP–BACE-1 interactions in axons, examining colocalization of APP/BACE-1 BiFC with organelle markers as above (**Fig. 4a**). Fluorescent puncta representing complemented APP/BACE-1 were seen throughout the length of the axon (**Fig. 4b**). However unlike dendrites, axonal APP/BACE-1 BiFC puncta largely colocalized with NPYss, a marker of Golgi-derived vesicles, and colocalization with endosomes was lower (**Fig. 4c**). Since dendritic APP/BACE-1 complementation was seen mostly in and around postsynaptic specializations where recycling occurs (**Fig. 3a**), we asked whether complementation

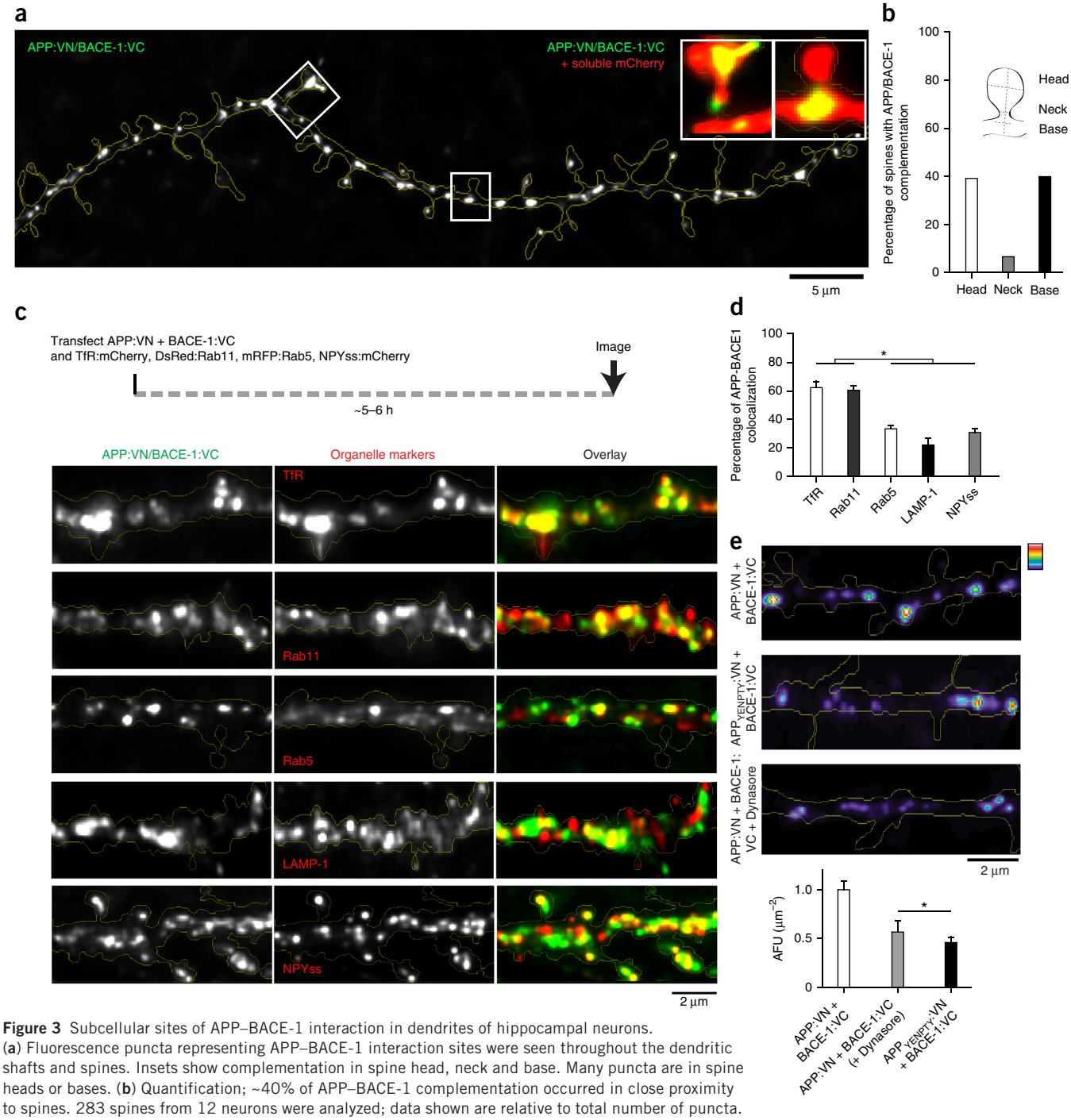

Figure 3 Subcellular sites of APP–BACE-1 interaction in dendrites of hippocampal neurons. (**a**) Fluorescence puncta representing APP–BACE-1 interaction sites were seen throughout the dendritic shafts and spines. Insets show complementation in spine head, neck and base. Many puncta are in spine heads or bases. (**b**) Quantification; ~40% of APP–BACE-1 complementation occurred in close proximity to spines. 283 spines from 12 neurons were analyzed; data shown are relative to total number of puncta. (**c**,**d**) To determine colocalization of APP–BACE-1 interaction sites with dendritic organelles, neurons were cotransfected with APP:VN/BACE-1:VC and the indicated organelle markers, and colocalization was determined quantitatively (see Online Methods). Complemented APP–BACE-1 particles most conspicuously colocalized with the recycling endosome markers TfR and Rab11 (~60%), and there was lesser (~30%) colocalization with early endosomal (Rab5), lysosomal (LAMP-1) and Golgi (NPYss) vesicle markers. 20–24 dendrites from 12–18 neurons in two separate cultures were analyzed; $^*P < 0.0001$, one-way ANOVA; error bars in **d**,**e** are mean ± s.e.m. (**e**) APP–BACE-1 complementation is also attenuated upon inhibiting clathrin-dependent endocytosis (by Dynasore) or by mutating an endocytosis motif in APP (APP_{YENPTY}). 18–25 dendrites from 10–14 neurons in two separate cultures were analyzed; $^*P = 0.0148$. AFU, arbitrary fluorescence units.

was also seen in presynaptic *en passant* boutons. The latter are major recycling sites in neurons and are mainly located along distal axons in our hippocampal cultures, where they can be easily identified by presynaptic markers[21]. To this end, we first cotransfected neurons with APP/BACE-1 and synaptophysin-mRFP, a marker for presynaptic boutons[21]. Almost all complemented APP/BACE-1 puncta colocalized with presynaptic boutons (**Fig. 4d**,**e**). To determine the relative enrichment of APP/BACE-1 BiFC at boutons, we used a quantitative algorithm ('targeting factor') that compares levels of transfected proteins at boutons to those in the flanking axon, normalizing for potential variations in expression levels (**Fig. 4f**; also see refs. 21,22). Presynaptic targeting of APP/BACE-1 BiFC was

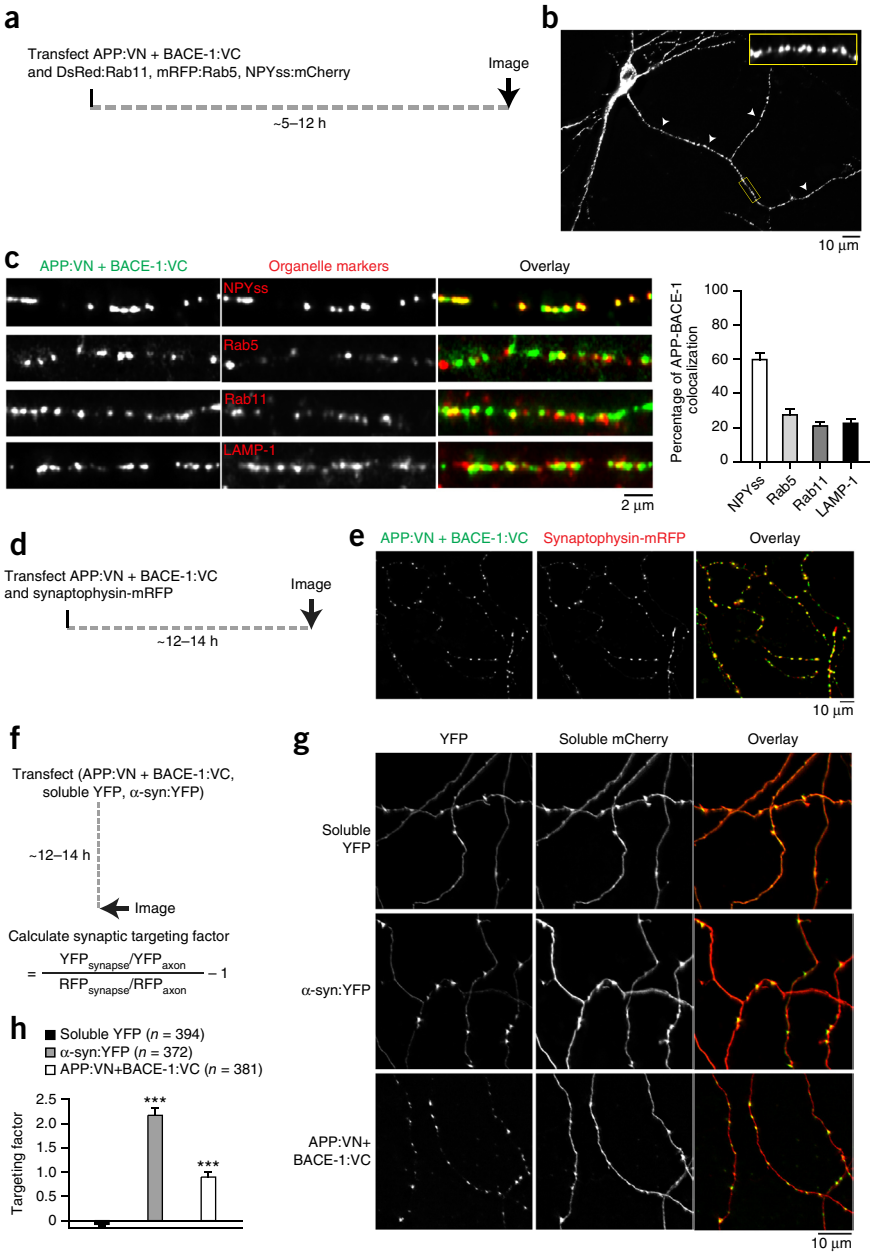

Figure 4 APP–BACE-1 interaction in axons and presynaptic boutons of hippocampal neurons. (**a**,**b**) To determine colocalization of APP–BACE-1 interaction sites with axonal organelles, neurons were transfected with APP:VN/BACE-1:VC and the indicated organelle markers, and colocalization was determined quantitatively (see Online Methods). Low-power view of APP/BACE-1 BiFC; arrowheads mark axon and box marks section magnified in inset. (**c**) Complemented APP/BACE-1 particles most conspicuously colocalized with NPYss, a marker for Golgi-derived vesicles, while colocalization with endosomal markers was limited. 20–25 axons in two separate cultures were analyzed. (**d**,**e**) To determine whether presynapses are sites of APP–BACE-1 interaction, neurons were cotransfected with APP:VN/BACE-1:VC and synaptophysin:mRFP (to mark boutons). ~96% of the boutons contained APP/BACE-1 BiFC. 257 boutons from 15 neurons in two separate cultures were analyzed. (**f**–**h**) Quantitative analyses of APP/BACE-1 BiFC presynaptic targeting, compared to the known presynaptic protein α-synuclein (α-syn). Neurons were transfected with the respective BiFC/YFP and soluble mCherry constructs and fluorescence at boutons was compared to that in flanking axons, normalizing for variations in expression. Representative images shown in **g**; data quantified in **h**. Presynaptic targeting of APP/BACE-1 BiFC at boutons was significantly higher than that of soluble YFP, though, as expected, not as high as that of α-synuclein. ~370–395 boutons from 20 neurons in two separate cultures were analyzed. *t*-test between soluble YFP and α-syn: YFP, $***P = 0.0001$; *t* test between soluble YFP and APP:VN + BACE-1:VC, $***P = 0.0001$; error bars are mean ± s.e.m.

significantly higher than that of a soluble marker, though it was, as expected, lower than that of a classic presynaptic protein, α-synuclein (**Fig. 4g**,**h**). These data suggest that APP and BACE-1 interact at presynaptic boutons.

The physical interaction of APP and BACE-1 in axons suggests that they might also be transported by a common carrier. To test this, we first examined the axonal transport of fluorescently tagged APP and BACE-1 individually and also determined colocalization of mobile APP or BACE-1 vesicles with organelle markers (**Fig. 5a**,**b**). Transport kinetics of APP- and BACE-1-containing vesicles were similar but not identical (**Fig. 5a**), and motile particles largely colocalized with NPYss, a marker for Golgi-derived vesicles (**Fig. 5b**). By contrast, colocalization of mobile axonal APP and BACE-1 vesicles with endosomal organelles was much lower (**Supplementary Fig. 3** and **Supplementary Table 1**). Finally, we asked whether APP and BACE-1 are cotransported in axons. To this end, we cotransfected neurons with APP:GFP and BACE-1:mCherry and examined their trafficking in axons by simultaneous dual-color imaging. Most moving APP vesicles (>80%) colocalized with BACE-1, but some BACE-1 vesicles were also transported independently (**Fig. 5c**).

Collectively, the above data indicate that most APP and BACE-1 are cotransported in hippocampal axons and that the enzyme-substrate pair can interact during transit. In further support of the latter, we found that complemented APP/BACE-1 BiFC particles in axons were also mobile (**Fig. 6a**,**b**). Unlike axons, complemented APP/BACE-1 BiFC particles in dendrites were largely immobile in mature (DIV 14) neurons, localizing in and around spines, as noted previously (**Fig. 6c**). Notably, APP/BACE-1 BiFC particles were mobile in younger (DIV 7) neurons lacking mature spines, suggesting that trafficking APP and BACE-1 can be 'captured' around dendritic spines, as shown previously for other proteins[23]. Complemented APP/BACE-1 BiFC particles at presynaptic boutons were also largely immobile, though moving particles were seen in flanking axons as expected (**Fig. 6d**).

Fate of endocytosed APP in neurons

A previous study tracked the fate of endocytosed BACE-1 in neurons, showing a remarkable retrograde bias of BACE-1-containing vesicles in dendrites[17]; however, the fate of endocytosed WT APP in neurons is less clear. To address this, we adopted a strategy whereby membrane-spanning proteins are surface-labeled using fluorescently

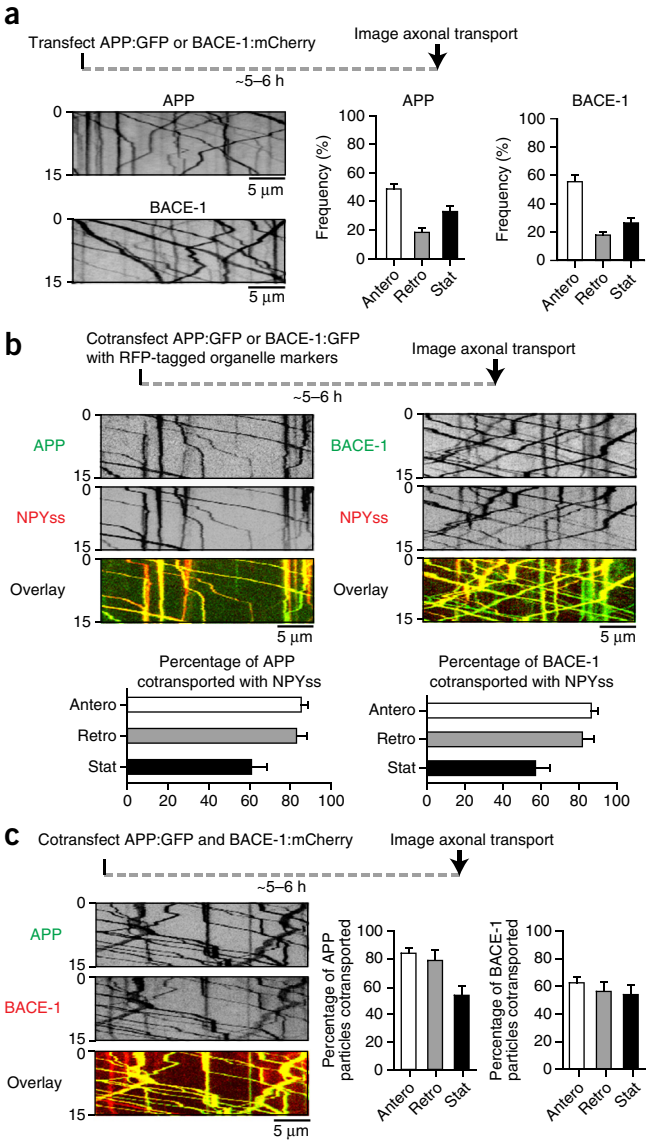

Figure 5 Axonal transport of APP and BACE-1. (**a**) Neurons were transfected with either APP:GFP (left panels) or BACE-1:mCherry (right panels), and axonal transport was analyzed at a high temporal resolution (see Online Methods). Schematic on top; representative kymographs with quantification shown below. Note similar kinetics of APP and BACE-1 transport. Estimated velocities of APP vesicles: anterograde (Antero), 1.74 ± 0.03 μm s^{-1}; retrograde (Retro), 1.51 ± 0.06 μm s^{-1}; and of BACE-1 vesicles: anterograde, 2.1 ± 0.06 μm s^{-1}; retrograde, 1.76 ± 0.07 μm s^{-1}. ~360 APP and 300 BACE-1 vesicles from 20–22 neurons in two separate cultures were analyzed. (**b**) Neurons were transfected with APP:GFP (or BACE-1:GFP) and various RFP-tagged organelle markers as noted and were examined live by simultaneous dual-color imaging. Schematic on top; representative kymographs with quantification shown below. Note cotransport with NPYss, a marker for Golgi-derived vesicles. For the APP–NPYss pair, ~320 APP and 390 NPYss particles were analyzed from 16–18 neurons in two separate cultures. For the BACE-1/NPYss pair, ~410 BACE-1 and 500 NPYss from 18–20 neurons in two separate cultures were analyzed. (**c**) Neurons were transfected with APP:GFP and BACE-1:mCherry and examined live by simultaneous dual-color imaging. Note that the majority of APP and BACE-1 particles are cotransported. All error bars are mean ± s.e.m.

tagged α-bungarotoxin (BTX)[24]. Specifically, we inserted a 13-amino-acid BTX-binding site at the N terminus of APP, after the APP signal sequence, to create BBS-APP; transfected neurons with BBS-APP; and then incubated the cultures with BTX-Alexa-594 (or BTX-Alexa-488) to label BBS-APP epitopes exposed to the dendritic surface (**Fig. 7a**,**b**). Internalized BBS-APP was seen throughout the somatodendritic compartment (**Fig. 7b**). BTX-Alexa-594 internalization was specific for BBS-APP and was not seen with an APP:GFP construct that lacked the BBS domain (**Fig. 7c**). Internalized APP particles were largely stationary, and mobile particles showed no directional bias (**Fig. 7d**), a behavior very different from the persistent retrograde kinetics reported for internalized BACE-1 (ref. 17).

What is the fate of endocytosed WT APP in neurons? To address this, we determined the colocalization of internalized APP with organelle markers. Neurons were transfected with BBS-APP and GFP-tagged organelle markers and incubated with BTX-Alexa-594, and colocalization of GFP with Alexa-594 was determined. In dendrites, a substantial fraction (~50%) of internalized APP vesicles were colocalized with TfR-positive recycling endosomes, while a smaller fraction (~25–30%) colocalized with Rab5 and NPYss (**Fig. 7e**,**f**). These results are reminiscent of the APP/BACE-1 BiFC data above. Surprisingly, however, a large fraction (~70%) of internalized APP colocalized with the late endosomal or lysosomal marker LAMP-1 (**Fig. 7f**). As lysosomes are not a major compartment where APP and BACE-1 interact (**Fig. 3c**,**d**), these data suggest an alternative route for internalized APP that might limit APP–BACE-1 interactions and APP cleavage (see Discussion). Internalized APP in neuronal cell bodies was distributed as puncta throughout the soma, colocalizing with both endosomal and TGN markers (40–50%), and colocalization with LAMP-1 (~80%) was again noted (**Supplementary Fig. 4**).

Reduced APP–BACE-1 interactions in a protective mutation

Recently, a search for low-frequency APP variants in whole-genome sequencing data from Icelanders revealed a mutation that confers protection against Alzheimer's disease (A673T, or the Icelandic mutation, henceforth called APP(Ice)[25]). Although studies suggest that the APP(Ice) mutation makes APP less susceptible to BACE-1 cleavage[26,27], the underlying mechanism is unclear. One might imagine that this mutation alters APP trafficking pathways, perhaps rerouting the protein into aberrant organelles, diminishing its affinity for BACE-1. Alternatively, physical approximation of the mutant protein to BACE-1 may be attenuated, perhaps as a result of conformational changes in the mutant protein. To study this, we synthesized an APP:VN construct containing the Icelandic mutation (APP(Ice):VN) and transfected it with BACE-1:VC into neurons (**Fig. 8a**). Fluorescence complementation was greatly attenuated (**Fig. 8b**,**c**), despite appropriate expression of the construct (**Supplementary Fig. 1**). Consequent β-cleavage of APP(Ice):VN was greatly diminished as well (**Fig. 8d**). To examine trafficking parameters of the APP(Ice) protein, we determined internalization of BBS-APP(Ice) using the BBS-BTX assay described above (**Supplementary Fig. 5a**). Internalization of BBS-APP(Ice) was similar to that of its WT counterpart (**Supplementary Fig. 5b**). Similarly, trafficking of APP(Ice):GFP was largely unaffected (**Supplementary Fig. 5c**). These data suggest that the protective effect of the APP(Ice) mutation may be a consequence of defective approximation of the enzyme-substrate pair before cleavage and not of altered vesicle trafficking. Finally, the OptiCAB assay also gave expected readouts in other cell types that can be easily propagated (**Supplementary Fig. 6**).

DISCUSSION

Subcellular locale of APP cleavage has been a topic of exceptional interest for decades, and yet precise sites where WT APP and BACE-1

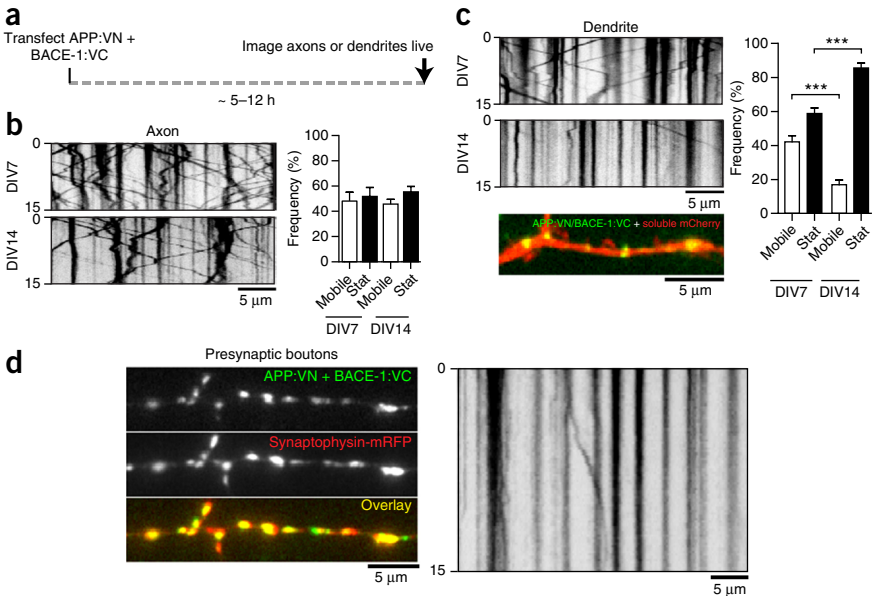

Figure 6 Kinetics of APP/BACE-1 BiFC particles. (**a**) Neurons were transfected with APP:VN and BACE-1:VC, and kinetics of complemented YFP particles were imaged live. (**b**) Representative kymographs (left) and quantification (right) of APP/BACE-1 BiFC movements in axons. ~200 (DIV7) and 160 (DIV14) vesicles from 12–14 axons in two separate cultures were analyzed; $P = 0.7488$ between the mobile groups and $P = 0.6634$ between the stationary (Stat) groups; *t*-test; error bars are mean ± s.e.m. (**c**) Representative kymographs (left) and quantification (right) of APP/BACE-1 BiFC movements in dendrites. Note restricted movement of APP/BACE-1 BiFC in regions around dendritic spines. ~200 (DIV7) and 170 (DIV14) vesicles from 12–14 dendrites in two separate cultures were analyzed. Image at bottom shows APP/BACE-1 BiFC in a dendrite. $^{***}P = 0.0002$ between the mobile groups and $^{***}P = 0.0002$ between the stationary groups; *t*-test; error bars are mean ± s.e.m. (**d**) APP/BACE-1 BiFC particles in presynaptic boutons were largely (85.19 ± 2.53%) stationary, with mobile particles comprising 14.79 ± 2.53%, as shown in the representative kymograph (right). ~150 YFP vesicles from 10–12 neurons in two separate cultures were analyzed; $P = 0.0001$, *t*-test.

meet in neurons have been essentially unknown. In this study we report optical assays to visualize the convergence and interaction of APP and BACE-1, and also to track internalized APP in hippocampal neurons. Our experiments provide the following insights, all in neurons. (i) They indicate that APP and BACE-1 interact in both biosynthetic and endocytic compartments. (ii) They implicate recycling microdomains such as dendritic spines and presynapses as important sites of APP–BACE-1 convergence (and thus β-cleavage). (iii) They indicate that recycling endosomes distributed throughout neuronal processes are a major locale of APP–BACE-1 convergence. (iv) They indicate that axonal APP and BACE-1 are cotransported in Golgi-derived vesicles and that they interact in these organelles. (v) They show that a substantial amount of APP endocytosed from the plasma membrane enters late endosomes or lysosomes—perhaps avoiding excessive cleavage. And finally, (vi) they suggest attenuated APP–BACE-1 approximation as a mechanistic basis for the Alzheimer's disease–protective Icelandic

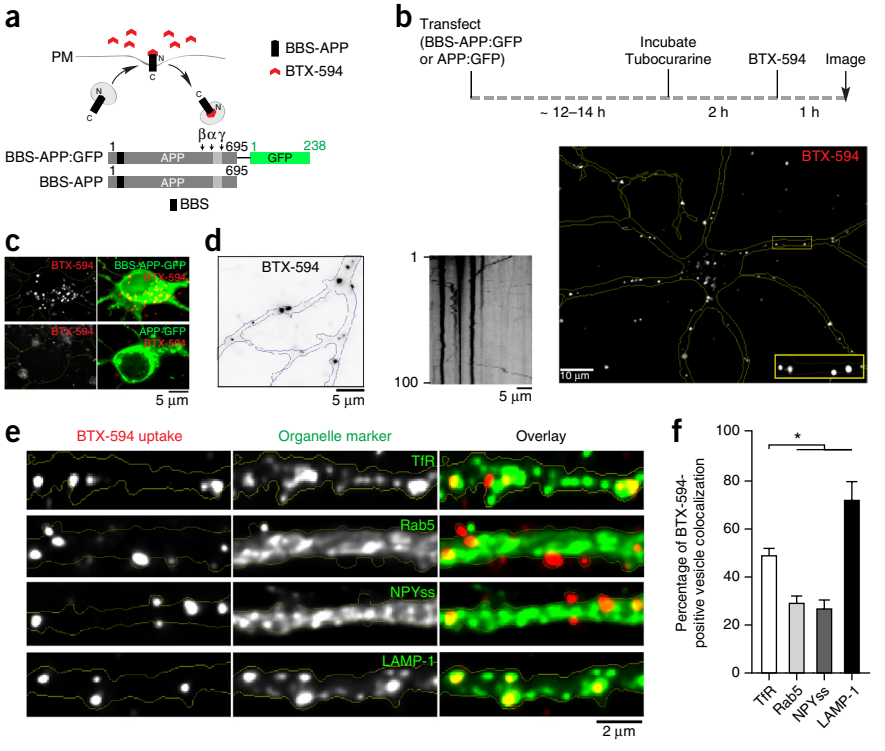

Figure 7 Fate of internalized APP in neurons. (**a**) Strategy of APP internalization assay. Neurons were transfected with an APP construct containing a BTX-binding site (BBS) at the luminal N terminus (BBS-APP), and cells were incubated with Alexa-594-labeled BTX (BTX-594). Upon recycling, BTX-594 binds to BBS-APP and internalized Alexa-594 dye indicates APP endocytosis. (**b**) Schematic shows experimental design; a representative neuron with internalized APP is shown below. Note APP internalization throughout somatodendritic compartments, magnified in inset. (**c**) Specificity of the BTX-594 uptake assay. BTX-594 internalization was seen in BBS-APP:GFP transfected neurons but not in neurons transfected with APP:GFP (lacking the BBS domain). Representative of 5–7 neurons in each group. (**d**) Internalized dendritic BBS-APP particles were most often stationary (54.8%) but also included particles exhibiting anterograde (24.7%) and retrograde (20.2%) motion. $N = 128$ particles from 12 neurons were analyzed; representative kymograph on right. (**e**,**f**) Colocalization of internalized BTX-594 with organelle markers. Neurons were transfected with BBS-APP and the stated organelle marker, and colocalization was analyzed in dendrites. Internalized BBS-APP predominantly colocalized with recycling endosomes and lysosomes (48.9% colocalization with TfR, 29% with Rab5, 26.7% with NPYss and 71.9% with LAMP-1; 18–22 dendrites from 15–18 neurons in two separate cultures were analyzed; $^{*}P = 0.0001$, one-way ANOVA. Error bars are mean ± s.e.m.

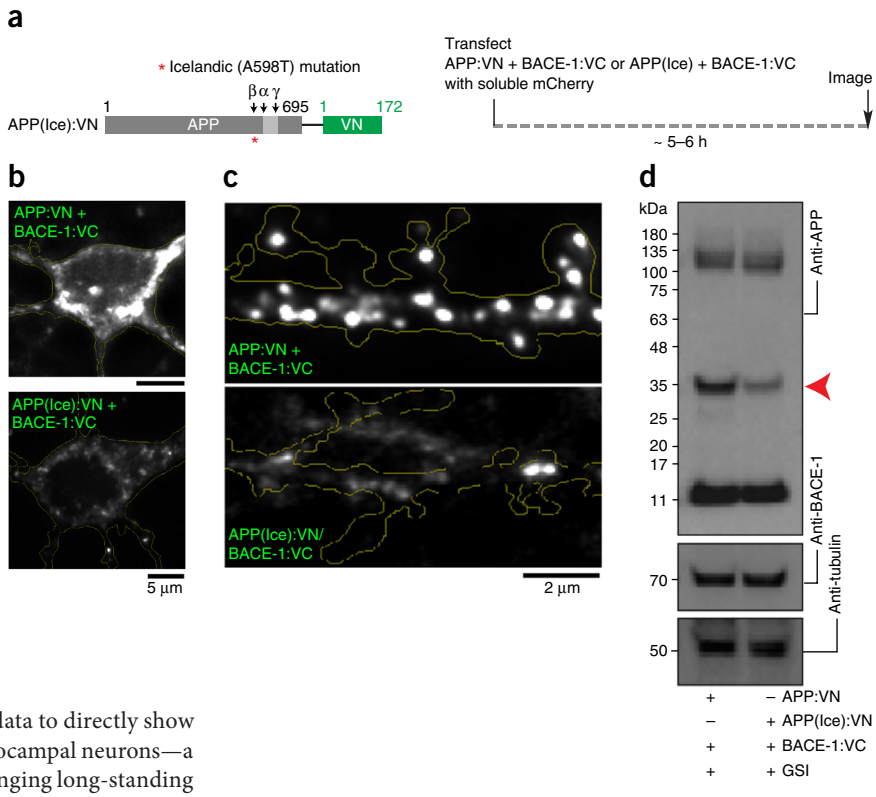

Figure 8 Attenuated APP–BACE-1 interactions with an Alzheimer's disease protective mutation. (**a**) Schematic showing location of Alzheimer's disease protective mutation, APP(Ice), and experimental strategy. (**b**,**c**) Neurons were transfected with APP:VN (WT or APP(Ice)) and BACE-1:VC, and fluorescence was analyzed. Complementation of APP(Ice) with BACE-1 was significantly lower in soma (normalized fluorescence intensity of APP(Ice):VN/BACE-1:VC was 0.22 ± 0.06 compared to APP:VN/BACE-1:VC, 1.0 ± 0.17; $P = 0.0001$, *t*-test) and dendrites (normalized fluorescence intensity of APP(Ice):VN/BACE-1:VC was 0.37 ± 0.07 compared to APP:VN/BACE-1:VC, 1.0 ± 0.18; $P = 0.0042$). 22–24 dendrites from 14–18 neurons in three separate cultures were analyzed. (**d**) BACE-1 knockout fibroblasts were cotransfected with APP:VN (WT or APP(Ice)) and BACE-1:VC, and APP fragments were analyzed by western blotting in the presence of γ-secretase inhibitor (GSI). The ~30-kDa band corresponding to the expected β-cleavage product of APP:VN (red arrowhead) was attenuated in the APP(Ice) lane (representative of four independent experiments).

mutation. To our knowledge, these are the first data to directly show interaction of this enzyme-substrate pair in hippocampal neurons—a cell-type relevant to Alzheimer's disease—challenging long-standing models of APP and BACE-1 trafficking based on studies in non-neuronal cells and providing concrete answers to controversies.

Somatodendritic organelles where APP is cleaved by BACE-1

Previous studies in HEK293T and other cell lines show that vesicles containing APP and BACE-1 internalized from the surface colocalize with early endosomes, suggesting that these organelles are the site of β-cleavage[4,28]. These data have led to the assumption that APP β-cleavage occurs mainly in early endosomal and not biosynthetic compartments[2]. However, other studies in cell lines suggest convergence of APP and BACE-1 at the TGN and multiple endosomal compartments, including early and recycling endosomes[5,6,29]. Regardless, the location of APP β-cleavage in neurons, the relevant cell-type in this context, has been unknown. Our experiments in hippocampal neurons suggest that, in the soma, WT APP and BACE-1 interact at the TGN. In dendrites, WT APP and BACE-1 largely interact in recycling endosomes (~60% colocalization of APP:VN/BACE-1:VC with TfR and Rab11), with lower levels of colocalization (~20–30%) with other endosomal markers (**Fig. 3**), thus implicating both biosynthetic and endosomal compartments in APP β-cleavage. Notably, about half of all APP–BACE-1 interactions were in and around dendritic spines (**Fig. 3a**,**b**). Indeed, these microdomains are rich in recycling endosomes that recycle with the plasma membrane of the spines[30], further supporting the concept that vesicle recycling is an important event in APP cleavage.

The collective data suggest that most steady-state WT APP–BACE-1 interactions in dendrites occur in neuronal recycling endosomes, though a transient association of APP and BACE-1 in early endosomes before their engagement in recycling compartments cannot be excluded. The potential discrepancies between data from non-neuronal cells and neurons are difficult to pinpoint, but principles governing APP trafficking in non-neuronal cells are not always applicable to neurons[1]. Neurons have an extensive network of highly dynamic and functional recycling endosomes extending throughout dendrites shafts and spines (refs. 7,30,31 and this study)—an anatomic feature that is obviously lacking in non-neuronal cells, where recycling endosomes are clustered around the nucleus[6,28]. Indeed, the dynamics of early and recycling endosomes in neurons is quite distinct, as we have reported previously[7]. Unlike early endosomes, recycling endosomes are much more dynamic and move with an anterograde bias in dendrites[7]. One might speculate that evolutionary demands of timely delivery into elongated processes have led to sophisticated endosomal networks in neurons that are very different from those in non-neuronal cells[32]. While studies in the latter have offered fundamental insights into the basics of APP processing, we reason that critical aspects in which neuronal pathways differ need to be appreciated as well. Finally, it is worth noting that neuronal recycling endosomes are acidic (ref. 31 and **Supplementary Fig. 7**); thus, these organelles provide a suitable milieu for BACE-1 enzymatic activity, optimal at low pH[33].

APP–BACE-1 convergence and trafficking in axons

Our live imaging data show that WT APP and BACE-1 are cotransported in axons and that they interact in these transport vesicles (**Figs. 4** and **5**). Previous studies have shown that APP is likely processed in axons and presynaptic sites[34–38]. It has also been suggested that APP and BACE-1 are cotransported in a common transport carrier[39], but this idea has been controversial[40–42]. However, arguments for or against cotransport of APP and BACE-1 have been largely based on biochemical or histological evidence, rather than direct, simultaneous visualization of the two proteins in living axons. Of note, one study did visualize axonal transport of APP or BACE-1 (separately) in axons of cultured retinal ganglion neurons, reporting much faster velocities for APP[43]. However, axonal transport of WT APP and BACE-1 was not simultaneously visualized, though qualitative data from mutant APP and BACE-1 suggested a lack of cotransport[43].

In our studies, simultaneous visualization of WT APP and BACE-1 trafficking in hippocampal axons clearly show that APP and BACE-1

were cotransported (**Fig. 5c**). Since our BiFC experiments showed that the two proteins also interact during transit, it is unlikely that they move in distinct but tandem vesicles that cannot be resolved by light microscopy. It also seems unlikely that these data are confounded by overexpression as, besides the short time-intervals after transfection (~5–6 h), overall kinetics of APP and BACE-1 were similar whether they were transfected individually or cotransfected in these neurons (**Fig. 5**). Our data also indicated that APP and BACE-1 interact in presynaptic boutons (**Fig. 4d–h**). The dichotomy between APP/BACE-1 trafficking in dendrites and axons is intriguing. While dendritic APP and BACE-1 largely move in distinct vesicles[7], they are cotransported in axons. The reasons are unclear at this time, but may be related to transcytosis[32].

Fate of internalized APP in dendrites

Though previous studies have examined internalization of APP in non-neuronal cells, the fate of internalized APP in neurons has been less clear. We used a technique whereby the intraluminal (extracellular) domain of a transmembrane protein is fluorescently tagged in live cells by surface labeling and the internalized tagged protein is then detected[24]. As predicted by our working model[7], internalized APP colocalized with recycling endosomes in dendritic shafts; notably, however, a large fraction (~70–80%) colocalized with late endosomes or lysosomes (**Fig. 7f**). APP and BACE-1 do not interact much in lysosomes (**Fig. 3c**,**d**), and BACE-1 is also not normally localized to these compartments[7], suggesting that routing of surface APP to late endosomes or lysosomes may be a mechanism by which APP enters the degradative pathway and escapes cleavage. This behavior is also consistent with the known short (~2 h) half-life of APP[44]. Accumulation of lysosomes in neurites and disruption of lysosomal pathways is an established pathology in Alzheimer's disease, and it is possible that such disruptions cause mislocalization of APP/BACE-1 in lysosomes, leading to enhanced cleavage in the acidic milieu. Alternatively, an intriguing possibility is that lysosomal accumulation in Alzheimer's disease is not a pathologic phenotype but an attempt by neurons to protect excess APP from cleavage. About half of the internalized APP in neuronal soma also colocalized with the TGN (**Supplementary Fig. 4**), consistent with the idea that retromers and endosomal sorting complexes required for transport (ESCRT) pathways recycle endocytic APP with the Golgi[14,29].

APP–BACE-1 approximation in a protective mutant

A recent study showed that a point mutation of APP in Icelandic populations is protective against Alzheimer's disease[25]. Understanding the mechanistic underpinnings of this mutation might lead to new ways of targeting Alzheimer's disease pathology, and at least two scenarios can be imagined. One is that the mutation might alter trafficking of the mutant APP, perhaps partitioning it into an aberrant organelle, and diminish interaction of the enzyme-substrate pair. The other is that trafficking routes might be unaffected but approximation of the two proteins before cleavage might be attenuated. Our experiments favor the latter scenario, suggesting that the APP(Ice) mutation attenuates the association of this protein with BACE-1 (and thus APP β-cleavage), without much effect on internalization and other trafficking parameters (**Fig. 8** and **Supplementary Fig. 5**). Recent studies also indicate that these mutations have additional effects on the aggregation properties of misfolded APP[26,27], suggesting multiple pathways by which this mutation protects against Alzheimer's disease. However, precise mechanisms by which the APP(Ice) mutation confers protection still remain unknown and may have to await a refined structural understanding of the underlying APP–BACE-1 interacting interface.

METHODS

Methods and any associated references are available in the online version of the paper.

Note: Any Supplementary Information and Source Data files are available in the online version of the paper.

ACKNOWLEDGMENTS

We thank G. Banker (Oregon Health and Science University) for the NPYss: mCherry and TfR:mCherry/GFP constructs, G. Patterson and J. Lipincott-Schwartz (NIH) for the GalT:mCherry/GFP constructs, Z.-H. Sheng (NIH) for the synaptophysin-mRFP construct, W. Almers (Oregon Health and Science University) for the broken CMV promoter and D. Boehning (The University of Texas Health Science Center) for the APP(Lon):GFP construct. Constructs from Addgene and investigators are acknowledged in the Online Methods. U.D. was partly supported by a pilot award from the UCSD Alzheimer's Center (P50 AG005131). This work was supported by grants from the NIH/NIA (R01AG048218 and NIH/NINDS (R01NS075233) to S.R.

AUTHOR CONTRIBUTIONS

U.D. and S.R. designed the assays and wrote the paper. U.D. designed and performed most of the experiments and data analysis. L.W. designed and performed the synaptic targeting and some of the axonal transport experiments. A.G. and L.W. helped with neuronal cultures and J.M.S. performed and analyzed some of the axonal transport experiments. S.L.W. and E.H.K. provided key reagents and technical advice.

COMPETING FINANCIAL INTERESTS

The authors declare no competing financial interests.

1. O'Brien, R.J. & Wong, P.C. Amyloid precursor protein processing and Alzheimer's disease. *Annu. Rev. Neurosci.* **34**, 185–204 (2011).
2. Rajendran, L. & Annaert, W. Membrane trafficking pathways in Alzheimer's disease. *Traffic* **13**, 759–770 (2012).
3. Kinoshita, A. *et al.* Demonstration by FRET of BACE interaction with the amyloid precursor protein at the cell surface and in early endosomes. *J. Cell Sci.* **116**, 3339–3346 (2003).
4. Sannerud, R. *et al.* ADP ribosylation factor 6 (ARF6) controls amyloid precursor protein (APP) processing by mediating the endosomal sorting of BACE1. *Proc. Natl. Acad. Sci. USA* **108**, E559–E568 (2011).
5. Greenfield, J.P. *et al.* Endoplasmic reticulum and trans-Golgi network generate distinct populations of Alzheimer β-amyloid peptides. *Proc. Natl. Acad. Sci. USA* **96**, 742–747 (1999).
6. Prasad, H. & Rao, R. The Na^+/H^+ exchanger NHE6 modulates endosomal pH to control processing of amyloid precursor protein in a cell culture model of Alzheimer disease. *J. Biol. Chem.* **290**, 5311–5327 (2015).
7. Das, U. *et al.* Activity-induced convergence of APP and BACE-1 in acidic microdomains via an endocytosis-dependent pathway. *Neuron* **79**, 447–460 (2013).
8. Kerppola, T.K. Design and implementation of bimolecular fluorescence complementation (BiFC) assays for the visualization of protein interactions in living cells. *Nat. Protoc.* **1**, 1278–1286 (2006).
9. de Virgilio, M., Kiosses, W.B. & Shattil, S.J. Proximal, selective, and dynamic interactions between integrin αIIbβ3 and protein tyrosine kinases in living cells. *J. Cell Biol.* **165**, 305–311 (2004).
10. Remy, I., Montmarquette, A. & Michnick, S.W. PKB/Akt modulates TGF-β signalling through a direct interaction with Smad3. *Nat. Cell Biol.* **6**, 358–365 (2004).
11. Citron, M., Teplow, D.B. & Selkoe, D.J. Generation of amyloid β protein from its precursor is sequence specific. *Neuron* **14**, 661–670 (1995).
12. Sahlin, C. *et al.* The Arctic Alzheimer mutation favors intracellular amyloid-beta production by making amyloid precursor protein less available to alpha-secretase. *J. Neurochem.* **101**, 854–862 (2007).
13. Muratore, C.R. *et al.* The familial Alzheimer's disease APPV717I mutation alters APP processing and Tau expression in iPSC-derived neurons. *Hum. Mol. Genet.* **23**, 3523–3536 (2014).
14. Small, S.A. & Gandy, S. Sorting through the cell biology of Alzheimer's disease: intracellular pathways to pathogenesis. *Neuron* **52**, 15–31 (2006).
15. Kaech, S., Huang, C.F. & Banker, G. Short-term high-resolution imaging of developing hippocampal neurons in culture. *Cold Spring Harb. Protoc.* **2012**, 340–343 (2012).

16. El Meskini, R., Cline, L.B., Eipper, B.A. & Ronnett, G.V. The developmentally regulated expression of Menkes protein ATP7A suggests a role in axon extension and synaptogenesis. *Dev. Neurosci.* **27**, 333–348 (2005).
17. Buggia-Prévot, V. *et al.* A function for EHD family proteins in unidirectional retrograde dendritic transport of BACE1 and Alzheimer's disease Aβ production. *Cell Reports* **5**, 1552–1563 (2013).
18. Koo, E.H. & Squazzo, S.L. Evidence that production and release of amyloid beta-protein involves the endocytic pathway. *J. Biol. Chem.* **269**, 17386–17389 (1994).
19. Perez, R.G. *et al.* Mutagenesis identifies new signals for β-amyloid precursor protein endocytosis, turnover, and the generation of secreted fragments, including Aβ42. *J. Biol. Chem.* **274**, 18851–18856 (1999).
20. Knowles, M.K. *et al.* Single secretory granules of live cells recruit syntaxin-1 and synaptosomal associated protein 25 (SNAP-25) in large copy numbers. *Proc. Natl. Acad. Sci. USA* **107**, 20810–20815 (2010).
21. Wang, L. *et al.* α-Synuclein multimers cluster synaptic vesicles and attenuate recycling. *Curr. Biol.* **24**, 2319–2326 (2014).
22. Gitler, D. *et al.* Molecular determinants of synapsin targeting to presynaptic terminals. *J. Neurosci.* **24**, 3711–3720 (2004).
23. Washbourne, P., Bennett, J.E. & McAllister, A.K. Rapid recruitment of NMDA receptor transport packets to nascent synapses. *Nat. Neurosci.* **5**, 751–759 (2002).
24. Sekine-Aizawa, Y. & Huganir, R.L. Imaging of receptor trafficking by using α-bungarotoxin-binding-site-tagged receptors. *Proc. Natl. Acad. Sci. USA* **101**, 17114–17119 (2004).
25. Jonsson, T. *et al.* A mutation in APP protects against Alzheimer's disease and age-related cognitive decline. *Nature* **488**, 96–99 (2012).
26. Benilova, I. *et al.* The Alzheimer disease protective mutation A2T modulates kinetic and thermodynamic properties of amyloid-β (Aβ) aggregation. *J. Biol. Chem.* **289**, 30977–30989 (2014).
27. Maloney, J.A. *et al.* Molecular mechanisms of Alzheimer disease protection by the A673T allele of amyloid precursor protein. *J. Biol. Chem.* **289**, 30990–31000 (2014).
28. Rajendran, L. *et al.* Alzheimer's disease beta-amyloid peptides are released in association with exosomes. *Proc. Natl. Acad. Sci. USA* **103**, 11172–11177 (2006).
29. Choy, R.W., Cheng, Z. & Schekman, R. Amyloid precursor protein (APP) traffics from the cell surface via endosomes for amyloid β (Aβ) production in the trans-Golgi network. *Proc. Natl. Acad. Sci. USA* **109**, E2077–E2082 (2012).
30. Park, M. *et al.* Plasticity-induced growth of dendritic spines by exocytic trafficking from recycling endosomes. *Neuron* **52**, 817–830 (2006).
31. Wang, Z. *et al.* Myosin Vb mobilizes recycling endosomes and AMPA receptors for postsynaptic plasticity. *Cell* **135**, 535–548 (2008).
32. Yap, C.C. & Winckler, B. Harnessing the power of the endosome to regulate neural development. *Neuron* **74**, 440–451 (2012).
33. Vassar, R., Kovacs, D.M., Yan, R. & Wong, P.C. The beta-secretase enzyme BACE in health and Alzheimer's disease: regulation, cell biology, function, and therapeutic potential. *J. Neurosci.* **29**, 12787–12794 (2009).
34. Buxbaum, J.D. *et al.* Alzheimer amyloid protein precursor in the rat hippocampus: transport and processing through the perforant path. *J. Neurosci.* **18**, 9629–9637 (1998).
35. Lazarov, O., Lee, M., Peterson, D.A. & Sisodia, S.S. Evidence that synaptically released beta-amyloid accumulates as extracellular deposits in the hippocampus of transgenic mice. *J. Neurosci.* **22**, 9785–9793 (2002).
36. Cirrito, J.R. *et al.* Endocytosis is required for synaptic activity-dependent release of amyloid-β *in vivo*. *Neuron* **58**, 42–51 (2008).
37. DeBoer, S.R., Dolios, G., Wang, R. & Sisodia, S.S. Differential release of beta-amyloid from dendrite- versus axon-targeted APP. *J. Neurosci.* **34**, 12313–12327 (2014).
38. Kandalepas, P.C. *et al.* The Alzheimer's beta-secretase BACE1 localizes to normal presynaptic terminals and to dystrophic presynaptic terminals surrounding amyloid plaques. *Acta Neuropathol.* **126**, 329–352 (2013).
39. Kamal, A., Almenar-Queralt, A., LeBlanc, J.F., Roberts, E.A. & Goldstein, L.S. Kinesin-mediated axonal transport of a membrane compartment containing beta-secretase and presenilin-1 requires APP. *Nature* **414**, 643–648 (2001).
40. Lazarov, O. *et al.* Axonal transport, amyloid precursor protein, kinesin-1, and the processing apparatus: revisited. *J. Neurosci.* **25**, 2386–2395 (2005).
41. Szodorai, A. *et al.* APP anterograde transport requires Rab3A GTPase activity for assembly of the transport vesicle. *J. Neurosci.* **29**, 14534–14544 (2009).
42. Sisodia, S.S. A cargo receptor mystery APParently solved? *Science* **295**, 805–807 (2002).
43. Goldsbury, C. *et al.* Inhibition of APP trafficking by tau protein does not increase the generation of amyloid-beta peptides. *Traffic* **7**, 873–888 (2006).
44. Ring, S. *et al.* The secreted beta-amyloid precursor protein ectodomain APPs alpha is sufficient to rescue the anatomical, behavioral, and electrophysiological abnormalities of APP-deficient mice. *J. Neurosci.* **27**, 7817–7826 (2007).

ONLINE METHODS

Constructs, antibodies and reagents. Venus N-terminal (VN, amino acid residues 1–172) and Venus C-terminal (VC, amino acid residues 155–238) fragments were PCR-amplified using an α-synuclein:Venus template[21] and cloned into pEGFP vector at AgeI and NotI sites, replacing GFP, to generate pVN and pVC plasmids. Human WT APP695 isoform and APP_{YENPTY} (described in ref. 7) were PCR amplified and cloned at HindIII and SacII sites of pVN to generate pAPP:VN and $pAPP_{YENPTY}$:VN. APP(1–636) was PCR amplified and cloned into pVN to generate APP-STOP40:VN. Mouse BACE-1 was cloned at XhoI and SalI sites of pVC to generate pBACE-1:VC. The Icelandic, Arctic and London APP mutations were generated by overlap PCR. Note that "APP(Ice)," "APP(Arc)" and "APP(Lon)" refer to the APP(A598T), APP(E618G) and APP(V642I) mutations in the APP-695 isoform used here and in other studies[26], and these correspond to the APP(A673T), APP(E693G) and APP(V717I) mutations, respectively, in the longest APP isoform (APP770; ref. 25). All spilt Venus constructs have a 10-amino-acid linker (PRARDPPVAT) between the gene of interest and the Venus fragments. To incorporate the BBS at the N terminus of APP, a SpeI site was introduced by A30T and E31S APP mutations. Annealed oligonucleotides for BBS sequence with SpeI sites at both ends were ligated to obtain pBBS-APP:GFP, pBBS-APP(Ice):GFP and untagged pBBS-APP. All constructs were cloned in-frame and fidelity was confirmed by sequencing.

The following constructs were obtained from Addgene: DsRed:Rab11a (cat. no. 12679, R. Pagano, Mayo Clinic); mRFP:Rab5 (cat. no. 14437, A. Helenius, ETH, Zurich; the GFP:Rab5 was made in-house by swapping the mRFP with GFP); LAMP-1:mCherry (A. Palmer, University of Colorado), and LAMP-1:GFP (cat. no. 34831, E. Dell'Angelica, UCLA). Antibodies used were as follows: APP (ab32136; Abcam), BACE-1 (MAB931; R&D), tubulin (clone DM1A; Sigma) and GFP (polyclonal, ab290; Abcam). Reagents were as follows: α-bungarotoxin Alexa-594 conjugate (Life Technologies), Alexa-594-transferrin (Life Technologies) and tubocurarine chloride (Tocris). Dynasore was used at a final concentration of 40 μM. All other reagents and culture media were obtained either from Sigma or Life Technologies.

Cell cultures and transfections. All animal studies were performed in accordance with University of California guidelines. Primary hippocampal neurons were acquired from postnatal (P0–P1) CD1 mice and transiently transfected using Lipofectamine 2000 as described previously[45]. Briefly, dissociated neurons were plated at a density of 50,000 cells/cm^2 on poly-D-lysine–coated glass-bottom culture dishes (Mattek) and maintained in Neurobasal/B27 medium with 5% CO_2. Neurons were cultured for ~5–6 h or ~12–15 h after transfection as described in the Results. For generating *Bace1*$^{-/-}$ cells, fibroblasts were cultured from the lungs of P1 *Bace1*$^{-/-}$– mice (obtained from Jackson Labs, from mice deposited by P. Wong, Johns Hopkins) followed by immortalization with SV40 t antigen. Both BACE-1 knockout and HEK293T cells (ATCC) were maintained in DMEM with 10% FBS and transiently transfected with the respective constructs using Amaxa 4D system with SF Cell Line 4D-Nucleofector X kit (V4XC-2024), programs CM137 and CM130, respectively, using the manufacturer's protocol. The cell density ranged from 1×10^7 to 3×10^7 cells/ml in a 100-μl transfection reaction. Cells were cultured for 24 h after transfection before analyses.

Microscopy, microscopy analyses and BTX uptake experiments. All images were acquired using an Olympus IX81 inverted epifluorescence microscope with a *z* controller (IX81, Olympus), a motorized *x-y* stage controller (Prior Scientific), a fast electronic shutter (SmartShutter), an ultrastable light source (Exfo Exacte) and CCD cameras (Coolsnap HQ2, Photometrics). Colocalization experiments were done as described previously[7]. Briefly, cells were transfected with desired constructs and fixed, and distal regions of the primary dendrites or first-order branches of secondary dendrites and axonal regions ~150 μm from the soma were selected for imaging. *z*-stack images were captured using a 100× objective with consistent imaging parameters (0.2 μm *z*-step, 500 ms exposure, 1 × 1 binning) and deconvolved (Huygens, Scientific Volume Imaging B.V.). Deconvolved *z*-stacks were subjected to a maximum intensity projection, resulting in 2D images for processing. Images were thresholded and colocalization was calculated as the fraction of area overlapping between the above-threshold structures in each image using custom algorithms written in Matlab (MathWorks). For live imaging, cells were transferred to Hibernate-E Low Fluorescence medium (HELF, BrianBits) at 35–37 °C (ref. 7).

For transport studies in dendrites, imaging parameters were set at 1 frame/s, total 200 frames and 500 ms exposure with 2 × 2 camera binning. Cargo dynamics in axons was imaged at 5 frames/s and 200 ms exposure (total of 75 frames, with no interval between frames) using the stream acquisition mode in MetaMorph. We found these imaging parameters to be critical for capturing all moving APP–BACE-1 cargoes, and lower time intervals led to an underestimation of particle kinetics. Axons were selected on the basis of criteria described in our previous studies[45,46]. For simultaneous two-color imaging, two spectrally distinct fluorophores were imaged using a Dual Cam imaging device (Photometrics) with 70% attenuation of the incident light to reduce photobleaching. Kymographs were generated in MetaMorph, segmental tracks were traced on the kymographs using a line tool, individual lines were saved as a .rgn file and the resultant velocity data (distance/time) was obtained for each track as described previously[45]. Analyses of all transport studies were done in a blinded fashion. For the BTX uptake experiments, neurons were pretreated with 150 μM tubocurarine chloride for 2 h before BTX-594 addition. After incubating with 7 μg/ml BTX-594 in Neurobasal/B27 medium for 1 h at 37 °C, cells were washed with ice-cold HBSS, pH 7.6, and fixed or imaged live in HELF imaging medium.

Quantitative imaging of presynaptic targeting. Cultured DIV13 hippocampal neurons (plating density of 60,000 cells/cm^2) were cotransfected with YFP (or VN/VC) tagged proteins (as described) and soluble mCherry using Lipofectamine 2000 and were imaged live 12–14 h after transfection. *z*-stack images were obtained and the targeting factor was calculated as described previously[21,22]. Briefly, fluorescence intensities for each channel were measured along lines drawn perpendicularly to the axons and across the boutons. Peak fluorescence along boutons and the adjacent axon were determined by fitting Gaussian functions to the resultant intensity profiles and corrected for background. Targeting factor was expressed as $[(YFP_{bouton}/YFP_{axon})/(RFP_{bouton}/RFP_{axon})] - 1$ (ref. 22). For colocalization analysis, boutons were identified and marked on synaptophysin:mRFP images and then the regions were transferred to YFP images to calculate the percentage of RFP boutons occupied by YFP.

Biochemistry. Neuro2A, HEK293T cells (ATCC) or BACE-1 knockout fibroblast cells were cultured for 24 h after transfection with DNA constructs using Amaxa 4D system and lysates were prepared in 50 mM NaCl, 50 mM Tris-Cl, 5 mM EDTA and protease inhibitor cocktail (Thermo Scientific), pH 8.0. After centrifuging at 1,000*g* for 20 min at 4 °C, supernatant S1 fractions were quantified and resolved by SDS-PAGE for western blot analyses.

Statistical analysis. Statistical analyses were performed using Prism software (GraphPad). Student's *t*-test (unpaired) or one-way ANOVA with Dunnett's *post hoc* test was used to compare two or more groups respectively. A *P*-value <0.05 was considered significant.

A **Supplementary Methods Checklist** is available.

45. Tang, Y. *et al*. Early and selective impairments in axonal transport kinetics of synaptic cargoes induced by soluble amyloid beta-protein oligomers. *Traffic* **13**, 681–693 (2012).
46. Ganguly, A. & Roy, S. Using photoactivatable GFP to track axonal transport kinetics. *Methods Mol. Biol.* **1148**, 203–215 (2014).